Monitoring Prostate Thermal Therapy with Diffusion-Weighted MRI

J. Chen[1,2], C. Diederich[3], M. van den Bosch[2], B. Daniel[2], G. Sommer[2], and K. Butts Pauly[2]

[1]Electrical Engineering, Stanford University, Stanford, CA, United States, [2]Radiology, Stanford University, Stanford, CA, United States, [3]Radiation Oncology, UCSF, San Francisco, CA, United States

Introduction MR-guided minimally invasive therapy has gain wide attention in recent years, a popular option of which is local hyperthermia therapy, including using high intensity focus ultrasound (1), laser (2), microwave (3) or radiofrequency (4) to elevate the temperature in the target tissue. The significant advantage of MR guidance over other imaging modalities is the ability to monitor the heat deposition and tissue viability *in vivo*. It has been shown that diffusion weighted MR imaging (DWI) provides a depiction of the thermal lesion in the prostate after cryoabablation (5, 6) and in uterine fibroids after HIFU (7). DWI is also well known to be temperature dependent (8), although due to its high motion sensitivity, *in vivo* study of DWI thermometry has been limited (9). The purpose of this work was to investigate the use of DWI for monitoring the evolution of the acute thermal lesion and to describe the implications for MR thermometry based on diffusion.

Method All animal experiments were approved by the Administrative Panel on Laboratory Animal Care. The heating was applied for ~15 min using an interstitial high intensity ultrasound applicator, with the amplifier power ranging from 5 W to 14 W, as marked in Fig.2. The MR imaging was performed on the 0.5T Signa SP open MRI system (GE, Milwaukee, WI). The body coil was used as the transmitter, and an endorectal coil was used as the receiver. Line scan diffusion weighted images (LSDI) (10) (TE/TR = 70/120 ms, matrix = 256×63, field of view = 24×6 cm, LSDI inclination angle = 70°, band width = 3.81 kHz, effective slice thickness = 7.3 mm, b = 10, 380 seconds/mm^2) were acquired during free breathing for the duration of the therapy. Diffusion trace data were calculated using three orthogonal gradient directions. The total scan time for each slice was 30 sec. About one hour after the completion of the heating, a triple dose of Gd-DTPA was administrated and a high-resolution T1-weighted sequence was performed to verify the heat induced lesion.

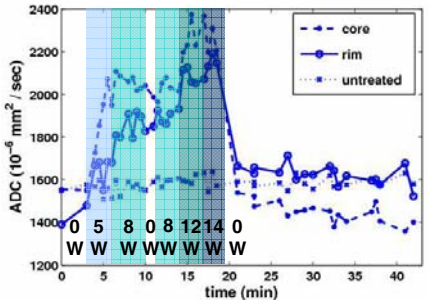

Fig.2 ADC time course of the whole procedure. The ADC value showed that the core had a higher temperature than the rim. Upon the completion of the heating, a thermal induced lesion presented in the core as a low ADC.

Results The heated region appeared as elevated ADC value on the ADC trace map, as shown in Fig.1 (a - c). As the heating continued, this region grew in volume and the ADC value kept increasing. Based on the Stokes-Einstein relationship between viscosity and the translational self-diffusion coefficient D, it was assumed that 1°C temperature change caused a 2.4% change in D. Using this assumption in ADC, the temperature map was calculated and superimposed onto the ADC map, as demonstrated in Fig.1 (e, f). After the whole prostate returned to body temperature, similar lesions presented on both the ADC trace map and contrast enhanced image, as illustrated in Fig.1 (d, g). Based on these results, three regions of interest (ROI) were chosen, one in the core of the thermal lesion, one ring shape ROI on the rim of the lesion, and another one in the untreated tissue. The ADC time courses of these ROIs are plotted in Fig. 2. During heating, the change of ADC closely followed the applicator power deposition, as marked in Fig. 2. It was observed that the ADC value dropped dramatically in both the core and the rim as soon as the applicator was powered off, but decreased faster in the core. To further demonstrate this phenomenon, one line of the ADC map through the center of the lesion is plotted as a function of time (Fig. 3). A signal intensity dip in the core (arrow head in Fig. 3) is seen early in the application of the heat and corresponds to the thermal lesion seen later.

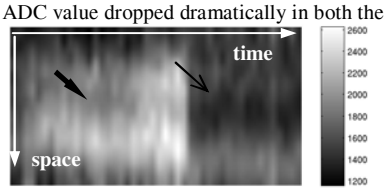

Fig.3 The evolution of the ADC value in one line across the lesion center. The dip (arrow head) during heating agreed well with the thermal lesion showed after the completion of the heating (arrow).

Conclusion and Discussion In this work we report an experimental study of using DWI to monitor an *in vivo* canine prostate thermal therapy with high intensity ultrasound. DWI was performed throughout the whole procedure with a temporal resolution of 30 sec under free breathing, and good correspondence between increased ADC value and power application was obtained. However, since the temperature-based ADC increase and the ADC change from tissue damage are competing effects, the calculated ADC-based temperature should be carefully interpreted. These temperature calculations may be accurate at low temperatures. However, the competing effects described here for the core of the thermal lesion mean that ADC-based temperature does not follow a simple linear relationship. Nonetheless, it is conceivable that the direct effects of thermal damage may be evaluated in real time through the use of diffusion-weighted MRI. In summary, DWI could potentially provide information of both temperature and tissue damage. Our future work includes correlating the DWI thermometry to proton resonance frequency method, further investigation of the use of the mixed information in treatment planning, and improvement in signal noise ratio and temporal resolution of diffusion weighted MRI.

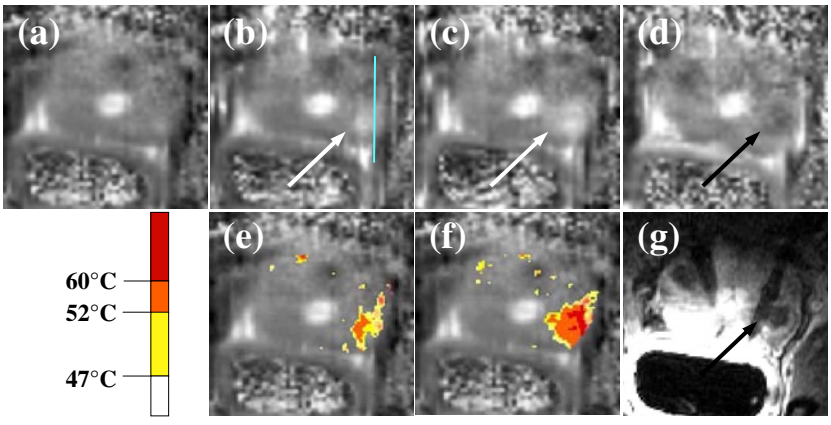

Fig.1 ADC trace map acquired before heating (a), at the beginning (b) and at the end of the heating (c), and at the end of the whole procedure (d). (e) and (f) are the color coded temperature maps calculated from (b) and (c). There is a clear correspondence between the heated region (white arrows) and the thermal lesion showed on the post-treatment ADC map (d) and the contrast enhanced T1-weighted image (g), pointed out by the black arrows.

Acknowledgement
NIH R01 CA077677, R01 CA111981, P41 RR009784

Reference

1) Cline et al, MRM 1993; 30:98–106
2) Germer et al, Surg Endosc 1998; 12:1317-25
3) Schwarzmaier et al, MRM 1995; 33:729-31
4) Samulski et al, Int J Hyperthermia 1992; 8:918-928
5) Butts et al, JMRI 2003; 17: 131-5
6) Chen et al, 14th ISMRM 2006, #196
7) Jacobs et al, Radiology 2005; 236: 196-203
8) Le Bihan et al, Radiology 1989; 171: 853-7
9) Macfall et al, Int J Hyperthermia 1995; 11: 73-86
10) Gudbjartsson et al, MRM 1996; 36: 509-19